

## Effects of nanosized metallic palladium loading and calcination on characteristics of composite silica<sup>①</sup>

WU Yur-cheng(吴玉程)<sup>1,2</sup>, WU Xia(吴 侠)<sup>1</sup>, LI Guang-hai(李广海)<sup>2</sup>, ZHANG Li-de(张立德)<sup>2</sup>  
(1. Faculty of Materials science and Engineering, Hefei University of Technology, Hefei 230009, China;  
2. Institute of Solid State Physics, Chinese Academy of Sciences, Hefei 230031, China)

**Abstract:** In order to investigate the effects of nanosized metallic palladium loading and calcination on the characteristics of composite silica, the silica was prepared by sol-gel technique, leading to an amorphous solid with mesoporosity, and the pore size distribution is narrow, centered at 3 - 5 nm. The composite silica was formed by impregnating palladium precursor into the porous network with sequel calcination in hydrogen. The results show that the nanosized palladium as guest phase in the composite silica is subjected to the mesoporous structure and calcination, resulting in the changes of optical adsorption that red-shifted to higher wavelength with the palladium loading and the heating temperature. The tailoring of the optical properties can be ascribed to the effect of the nanosized metal particles and interactions occurred between palladium and silica.

**Key words:** nanosized palladium; silica host; nanocomposites; calcination

**CLC number:** TB 383

**Document code:** A

### 1 INTRODUCTION

The motivation for the research on colloidal metal particles stemmed from their unique electro-optical and electrochemical properties<sup>[1-3]</sup>. During the past few years, a flurry of activity has been directed towards the preparation of nanosized metallic particles due to large enhancement in the physical properties of nanostructured composites compared to the bulk<sup>[4-6]</sup>. Therefore, size-dependent changes in band-gap energy, excited-state electronic behavior and optical spectra are generated drastically from those known for the molecular and bulk limits, respectively. Dispersions of nanoparticles afford accurate tuning for optical, electrical, and magnetic properties of many types of inorganic solids. For instance, the dispersion of metallic particles in an insulating matrix gives rise to materials in which the electric resistivity varies with the metal content and a transition from the metallic to the insulating regime is observed when a percolation network is obtained<sup>[7-10]</sup>. Traditionally, composites have been fabricated from preformed composites in a process that organizes them in a matrix, and with a particular arrangement. However, the nanostructured composites exert the nanosized dispersions in a matrix with special structure leading to the tailored functions<sup>[11, 12]</sup>. The mostly investigated composites<sup>[13-15]</sup> were some noble metals (Au, Ag, Pt) and transition metal elements (Pd, Fe, Co and Ni) embedded into

the oxide matrix.

Metal particles dispersed in an inorganic oxide can be obtained by various physical and chemical techniques, including metal evaporation decomposition of metal compounds and photo chemical or chemical reduction of metal complexes<sup>[16]</sup>. Sol-gel method has been used to create composites obtained by the incorporation of small metal or oxide particles in non-metallic matrices<sup>[17]</sup>, so that this method makes it possible for the introduction of various concentrations of different components in a matrix with molecular homogeneity, which can be vitreous or crystalline, either porous or densified, and hence their compositions are more controllable. Silica gels are usually prepared from the solution containing the mixture of tetraethosilane, ethanol and water based on the hydrolytic polycondensation reactions, leading to the formation of the silica network converted from three-dimensional polymer molecules with large specific surface area and narrow pore size distribution<sup>[18]</sup>. They have many advantages that acted as a matrix for the synthesis of nanometer dispersed phase, which offers the possibility for new catalytic and magnetic materials, exhibiting high activity and selectivity or novel magnetic characteristic<sup>[19, 20]</sup>.

Palladium, an active metal, with nanoscale can be prepared by different means, leading to various applications from catalysis to electronics<sup>[21, 22]</sup>. For the palladium composite, the properties to quite a lot ex-

① **Foundation item:** Project(00046403) supported by the Natural Science Foundation of Anhui Province, China; project(G19990645) supported by the National Key Fundamental Research and Development Program of China

**Received date:** 2003 - 01 - 09; **Accepted date:** 2003 - 06 - 03

**Correspondence:** WU Yur-cheng, Professor, PhD; Tel: + 86-551-2901365; Email: yewu@issp.ac.cn

tent depend upon the state of palladium and the interactions with the matrix. The influencing factors to the properties of the composite can be ascribed as the size distribution of the metallic particles and/or the pore structural features, and the preparation and characterization of palladium composite are critical for a fundamental understanding and tailoring of materials properties of practical use. It is well known that the introduction of the metal phase in the sol during the gelation allows the metal to have a direct interaction with the silica matrix<sup>[23]</sup>. However, in this paper, we prepare nanosized palladium/silica gel composites by impregnating the palladium precursor into porous silica previously made, and the evaluation on the relationship between the microstructure and optical property is performed. The effect of palladium loading and calcination on the pore structural characteristics of the resulting silica composites is presented.

## 2 EXPERIMENTAL

The preparation for the nanosized palladium/silica has been processed in following way. Reagent grade tetraethyl silicate (TEOS) was used as the starting material, and the solutions were prepared in molar ratio of TEOS: EtOH (solvent): water: catalyst = 1: 4: 24: 0.02. The deionized water was added dropwise to TEOS and EtOH and was stirred together in room temperature. HNO<sub>3</sub> as catalyst was added for hydrolysis to maintain the pH value at 1.5 – 2 during stirring. Then the sol was cast into 30 mm glass Petri dishes after complete homogenization, and covered with a polyethylene sheet and kept at 60 °C to gel. After gelation and drying at the same temperature for two weeks, the aged bulk gels were thermally treated stepwise in a case electric furnace at 100 – 600 °C for 2 h. The rate of heating was sufficiently small to keep the monolithic aspect of the gels and avoid a temperature gradient inside a sample that can cause heterogeneity in gel properties or the formation of cracks in gel. The treatment was chosen as a reasonable compromise between the need for eliminating the solvents and the organic molecules trapped in the gel network, so the transparent gel-silica monolith with different structural features was obtained for the synthesis of nanometer palladium. The bulk colorless silica was immersed into a 100 mL solution with concentrated amounts of H<sub>2</sub>PdCl<sub>4</sub> as palladium precursor designated as 0.1, 0.2 and 0.5 mol/L, and the solution was vigorously stirred to promote the introduction of palladium. The resulting silica was still transparent with slight yellow color indicating that the palladium precursor was indeed assembled into the porous media. We are interested in obtaining palladium

nanoparticles, the final step will be the reduction of the metal ions which is generally carried out by fluxing the gel with H<sub>2</sub> at 400 °C and 600 °C. Also can the same routes be performed for the nanocomposite coatings using the dipping technology.

BET method was used to characterize the pore structure and the pore size distribution, as well as indirectly to reflect the size scale of metallic palladium. The distribution of pore size up to 20 nm diameter was determined from N<sub>2</sub> adsorption isotherms. The isotherms were measured with an Omnisorp 100CX apparatus to get the surface area and the distribution of pore size. X-ray diffraction (XRD) characterization was performed in a MAP18AHF diffractometer (MAC Science Co. Ltd.) using CuK<sub>α</sub> radiation and Ni filter at a scan rate of 8(°)/min, operating at 40 kV and 100 mA. H-800 transmission electron microscope (TEM) was used to observe the size and distribution for the silica and the nanosized dispersion in bright-field image. The UV-Vis spectra were recorded in a Cary 5E UV-VisNir spectrophotometer over the wavelength of 200 – 2500 nm.

## 3 RESULTS AND DISCUSSION

### 3.1 Characterization of mesoporous silica gels

The X-ray diffraction patterns of the silica are shown in Fig. 1. The diffraction at 2θ = 22.12° intensified to the maximum with broad spreading towards both sides. It is obviously characterized as a typical amorphous structure. The patterns between prepared state and sintered state can be compared with nearly same features, as the sintering only gave rise to the evaporation of the residual organics and strengthening of the network except for the structure.

The pore structure and pore size distribution of the SiO<sub>2</sub> can be measured by the surface areas together with porosity analysis instrument. The hysteresis loop in the adsorption-desorption isotherm of the silica formed with different pressures is shown in Fig. 2, indicating that the solid characterized as porous network with mesoporosity. We can infer the mesoporous structure as IV type like an “ink-bottle” according to the shape of the loop<sup>[24]</sup>.

According to the formula  $(P/P_0)/[V(1 - P/P_0)] = 1/(V_m C) + (C - 1)(P/P_0)/(V_m C)$ <sup>[25]</sup>, we analysed the mesoporous features and got the BET linear curve plotted as  $10^3 X/[V(1 - X)]$  vs  $X$  (assumed  $P/P_0 = X$ , ranged from 0.05 to 0.25), as shown in Fig. 3. Using the intercept of BET plot as  $0.15 \times 10^{-3}$  and the slope  $8.98 \times 10^{-3}$ , the surface areas of silica in prepared state was calculated as 476.28 m<sup>2</sup>/g.

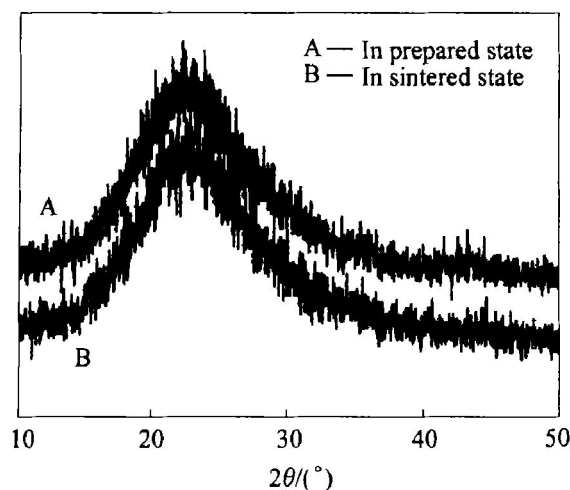


Fig. 1 XRD of silica gels in different states

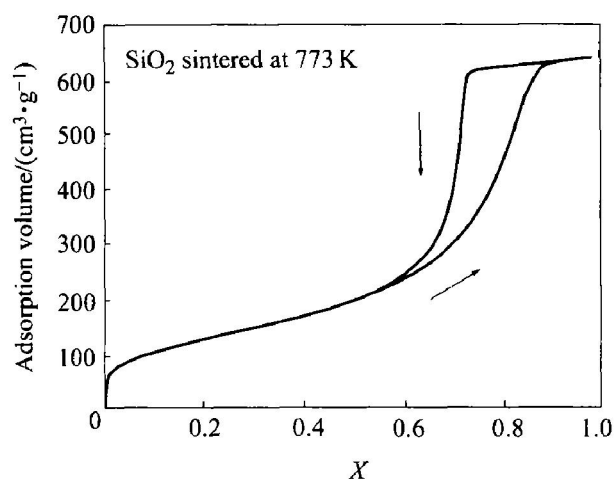


Fig. 2 Changes of adsorption volume with pressure for silica gel

The adsorption volume can be used to represent the pore volume. The distributions of the pore size are shown in Fig. 4. The whole pore volume is 1.019 2 mL/g with distributed pore size higher than 1 nm, the pore diameters in the range of 6 ~ 8 nm are relatively concentrated with 81.28%, 2 ~ 3 nm only 10.77%. It can be concluded that the pore diameters centered at 6 ~ 8 nm, indicating the pores having narrow size distribution.

### 3.2 Nanosized palladium particles in gel composites

Fig. 5 shows the adsorption and desorption isotherms for  $\text{SiO}_2(1)$  and  $\text{Pd}/0.2\text{M}/\text{SiO}_2(1)$  composite, which also have the same IV-type isotherm as the silica with a  $\text{N}_2$  hysteresis loop at different opening and closing pressures, showing the palladium composites have the identical mesoporous structural features. As palladium precursors impregnated into  $\text{SiO}_2$  matrix, they occupy some sites and block the flow of nitrogen inside the interlinked pores leading to a decrease in adsorption volume for the resultant composite. The changes

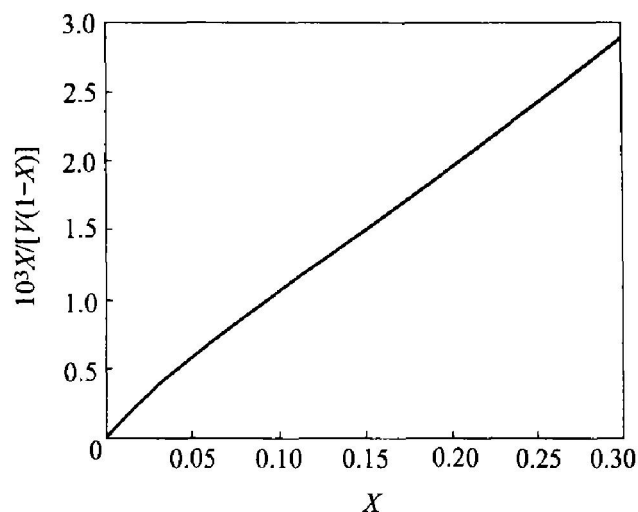


Fig. 3 BET linear relation of porous silica

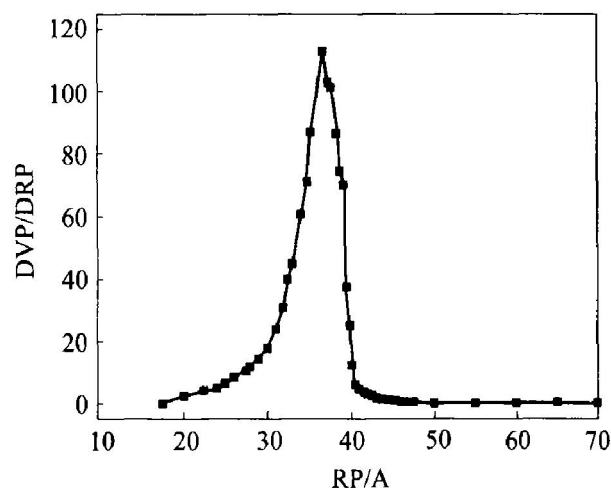


Fig. 4 Distribution of pore size of silica gel

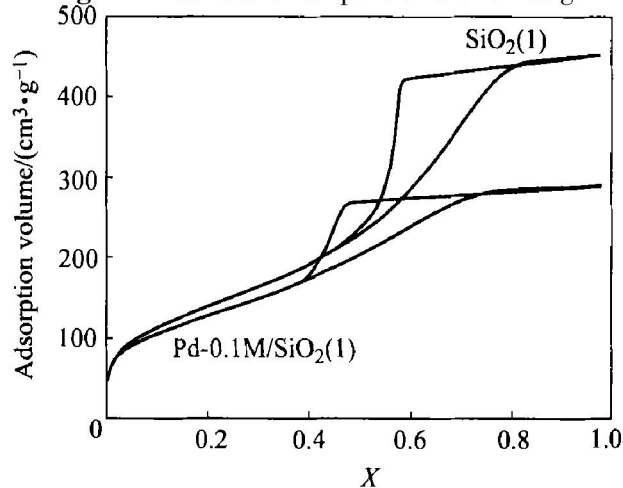


Fig. 5 Adsorption isotherms of silica gel and composites

also demonstrate the existence of metallic palladium into the porous matrix and the formation of  $\text{Pd}/\text{SiO}_2$  composite. The adsorption volume decreases further with increasing the loading of palladium. Contemporary, the nitrogen adsorption also provides information on the surface and pore size distribution for the mesoporous silica system.

The X-ray diffraction patterns of palladium composites treated at different atmosphere are shown in

Fig. 6. The diffraction of the composites calcined at 400 °C in hydrogen becomes evident due to the formation and growth of nanosized palladium. However, the pattern for the composite treated in oxygen atmosphere nearly keeps the same as that of amorphous silica matrix. It can be explained that palladium oxide is not diffracted in comparison with the metal palladium in the silica.

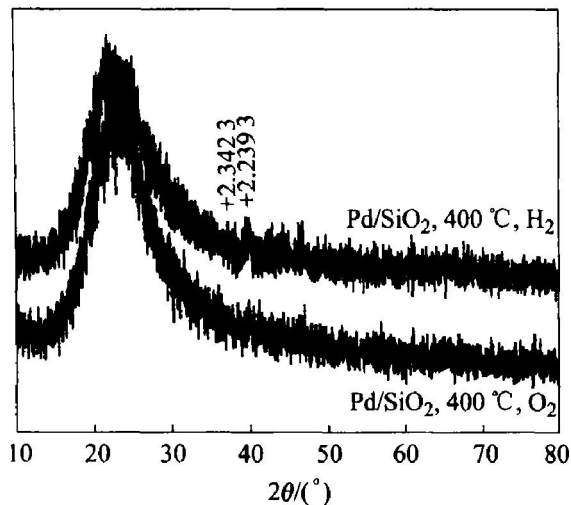


Fig. 6 XRD of nanosized palladium composites

### 3. 3 Effect of nanosized palladium loading on mesoporous structure of composites

The pore size distribution is obtained using the equation from the adsorption branch of the isotherm, as shown in Fig. 7. The silica is produced with two kinds of pore size distribution centered at 3.5 and 4.5 nm, respectively, labeled as SiO<sub>2</sub>(1) and SiO<sub>2</sub>(2). The introduction of metallic palladium gives rise to a change in the pore size distribution for the composites, but no evidence can be found the change of the based pore structure that the matrix existed previously, suggesting that the metallic palladium merely located in the pores. The result is consistent with the change of N<sub>2</sub> adsorption volume for the pure silica and palladium composites. It can be known that the behavior of metallic palladium is restricted to the porous matrix.

The thermal treatment generally promotes the conglomeration of the guest phase along the interlinked pores<sup>[26]</sup>. However, silica can be once more subjected to a higher temperature, because it has been pretreated at 600 °C for removal of the residues and rigidity of the three-dimensional network. Accordingly, the re-treatment below 600 °C will not affect the structure for the pure silica and the composites. On the contrary, relative broad distribution for Pd/SiO<sub>2</sub> composites prepared through direct mixing of precursor in silica sol was observed<sup>[27]</sup>, further indicating the advantage of impregnation method that can endure the metallic palladium uniformly dispersed into the matrix, leading to a cage effect for the nanosized dispersed

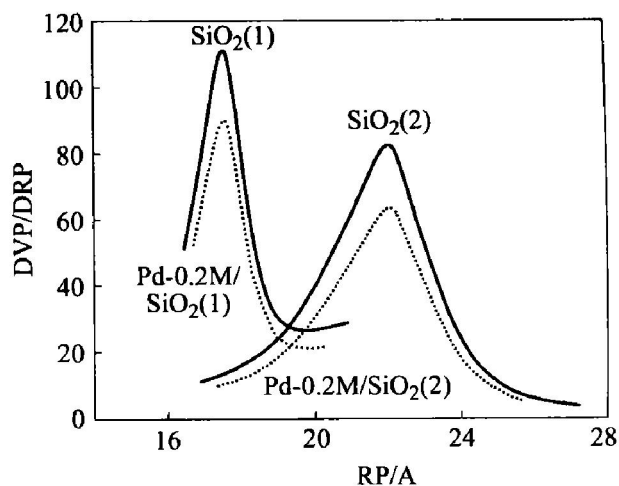
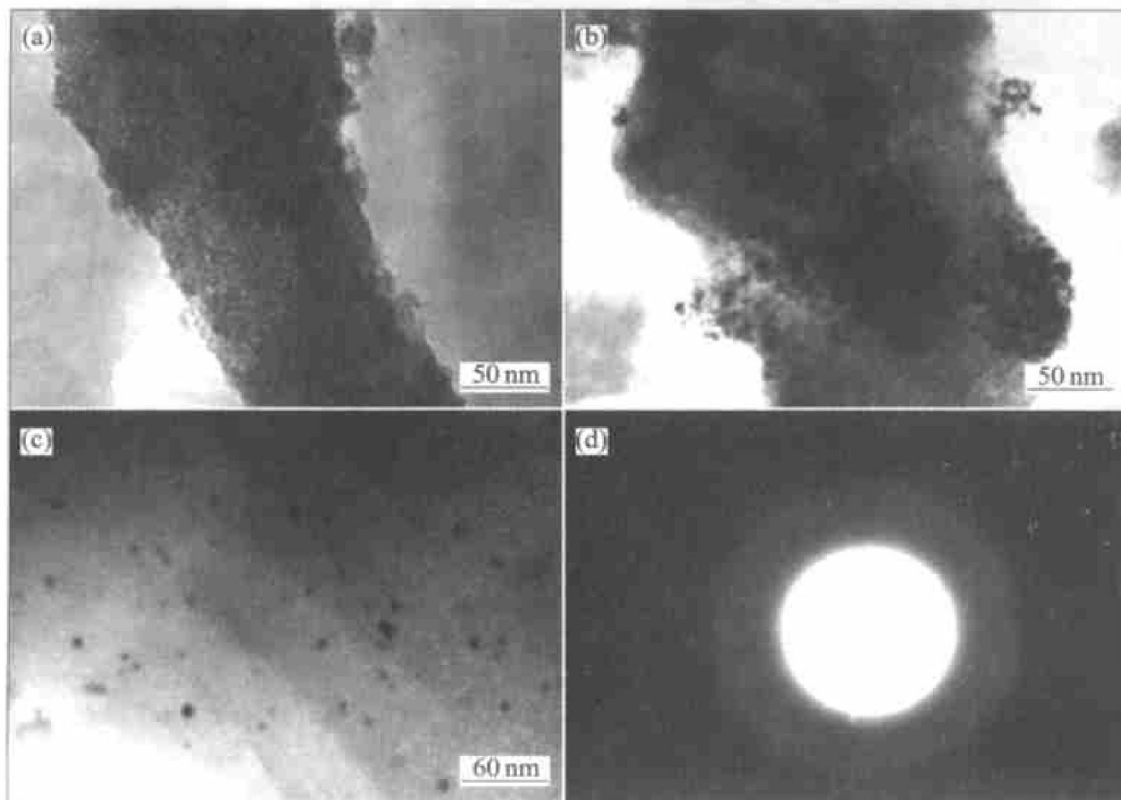


Fig. 7 Effect of size distributions of silica matrices on nanosized palladium composites

phase. The studied porous silica finds the surface areas ranging 500 – 800 m<sup>2</sup>/g, depending on the ratio of each component, gelation temperature and sintering process. After impregnation of metallic palladium, the surface area results of the composites show the lower values compared to the pure silica. It is worth to mention that the surface area values of the composites can not represent a true surface area of metallic palladium, because they are calculated according to the pore volumes of the silica matrix that were partly decreased due to palladium inhabited in the pores. It is undoubtedly to know that the characteristics of palladium are related to the size, and the surface area is mainly dependent of the size. Thus, the slight decrease in surface area of the composites is not enough considered, and the size of palladium in the matrix is the most important and can be restricted by the porous cage.

TEM micrographs and XRD spectra showed the presence of very small palladium particles homogeneously distributed in the silica matrix. Fig. 8 shows the micrographics for the silica and the composites. It can be found from TEM observations in powder samples to be 3 – 4 nm in size for SiO<sub>2</sub>(1), and the most of palladium particles are dispersed within the SiO<sub>2</sub> matrix and that their size distribution is very narrow about 5 – 7 nm (Pd-0.2M/SiO<sub>2</sub>(1)). The average size of palladium particles calculated from measurements on the TEM micrograph is distributed about 5 – 10 nm according to the histogram. It is almost identical with the BET results. With increase in the loading of palladium, the obvious change in size was not observed. The tendency of aggregation for palladium particles in the composite is confirmed after heat treatment at 600 °C, shown as Fig. 8 (C). As a result, the composite results in a broader size distribution that can not be identified definitely from the BET result



**Fig. 8** TEM micrographics of the porous  $\text{SiO}_2$ (a), and the nanosized  $\text{Pd}0.5\text{M}/\text{SiO}_2(1)$  composites in prepared state(b), heated at  $600\text{ }^\circ\text{C}$  in hydrogen(c) (bright field image), and(d) diffraction pattern

above, but the electron diffraction (Fig. 8(D)) still show the amorphous feature indicating the palladium particles are quite small. X-ray diffraction patterns show a halo pattern for all composites, characterized as amorphous silica, because the palladium loading is much less compared to the silica matrix. The extension of the method to larger pore size produces bigger metal particles and an increasing spreading of size, that is, the increase of the metal content produces a more significant growth of particle dimensions and a broadening of particle size distribution.

### 3. 4 Effects of nanosized palladium loading and heat treatment on optical properties of composites

The UV-Vis spectroscopy was recorded in order to get more information about the effect of palladium in the matrix. The UV-visible and near-IR adsorption spectra of the resulting nanosized composites depending on the loading of palladium and heated temperature are shown in Fig. 9. It can be found that, the nanosized composites give rise to the band at low energy that has dramatically changed position and adsorption profile in comparison with the pure silica. The adsorption spectra of the composites reveal a red-shifted band to longer wavelength range with the increase of the loading of palladium. From the value of the pure silica

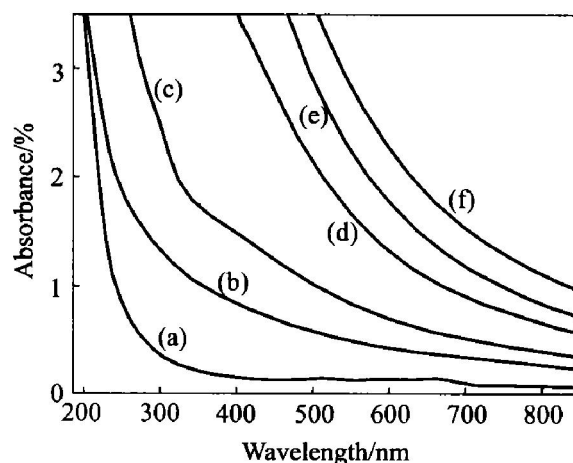


**Fig. 9** UV-VIS spectra of porous silica and nanosized composites with (a)  $\text{SiO}_2(2)$ , (b)  $\text{Pd}0.1\text{M}/\text{SiO}_2(2)$ , (c)  $\text{Pd}0.2\text{M}/\text{SiO}_2(2)$ , (d)  $\text{Pd}0.5\text{M}/\text{SiO}_2(2)$  in prepared state, (e)  $\text{Pd}0.5\text{M}/\text{SiO}_2(2)$  heated at  $400\text{ }^\circ\text{C}$  and (f)  $\text{Pd}0.5\text{M}/\text{SiO}_2(2)$ ,  $600\text{ }^\circ\text{C}$  in  $\text{H}_2$

$\text{SiO}_2(2)$ , the adsorption edges for  $\text{Pd}0.1\text{M}$ ,  $\text{Pd}0.2\text{M}$  and  $\text{Pd}0.5\text{M}$  in  $\text{SiO}_2(2)$  are located at 287, 364 and 590 nm, respectively. This suggests the presence of the palladium and interaction between the matrix and introduced phase. With decreasing palladium content, the adsorption threshold shifts towards to a lower wavelength region because of size quantization effect and surface effect of small particle<sup>[28]</sup>. The



size of palladium nanoparticles in the composites is shown above and increases with the loading of the precursor because the opportunity of the small particle growth is increased in the limited range of the pores. Evidently, a characteristic blue shift occurs with decreasing size of palladium particles. The Pd/SiO<sub>2</sub> composites change from colorless to brown-yellow and gradually become deep with palladium loading.

When the nanosized composite Pd-0.5M/SiO<sub>2</sub> (2) is subjected to the heat treatment, the color tends to be grey-brown which is attributed to the growth and change of surface state of the small particles. The heatings at 400 and 600 °C result in changes in the UV-Vis spectra, exhibiting that the adsorption band of the composite is further red-shifted to higher wavelength with temperature. The increase of spectral absorbance during heat treatment corresponds to the known spectral behavior of nanostructured composites. Such small metallic particles expose a high optical absorbance due to the existence of discrete energy levels of electron and particularly of specific surface states.

These observations suggest that the thermal formation of the high spectral absorbance were not caused by the matrix, but by the behavior of the metal particles. When the metal loading and heating temperature increase, the nanostructured composites lead to the interface interactions between the particles or the matrix and metallic phase, which become evident with the size of the particles. We assume that the particle size increases with high loading and high heating temperature. Further theoretical study is required in order to quantitatively understand the change of the adsorption spectrum that depends significantly on the metal loading and heat treatment.

#### 4 SUMMARY

The porous silica can be prepared using sol-gel technique leading to different structures that are controlled by some components and operating parameters. The assembled nanosized palladium into the porous network could not result in the changes in the matrix structure but some other features such as pore size and distribution as well as surface areas. The loading of palladium found to be 5–10 nm in size depending upon the porous structure and calcination, gives rise to the optical absorption red-shifted to higher wavelength that enhanced further with heating temperature.

#### ACKNOWLEDGEMENTS

Dr. ZHANG Yong and Dr. SONG Guang-ming in Institute of Solid State Physics and Institute of Intelligent Machinery, Chinese Academy of Sciences are gratefully acknowledged for their much help during experiments. The authors also thank the help in the

experiment and the English writing of this paper to Dr. W. Sprengel (ITAP, University of Stuttgart, Germany) during his visiting to ITAP in 2001–2002.

#### REFERENCES

- [1] de Tacconi N R, Wenren H, Mcchesney D, et al. Photoelectrochemical oxidation of formate ions on nickel-titanium dioxide nanocomposite electrodes [J]. *Langmuir*, 1995, 14: 2933–2935.
- [2] Li T, Moon J, Morrone A A, et al. Preparation of Ag/SiO<sub>2</sub> nanosize composites by a reverse micelle and sol-gel technique [J]. *Langmuir*, 1999, 15: 4328–4334.
- [3] Lee M, Lee C, Lee K C. Microstructure and surface plasmon absorption of sol-gel prepared Au nanocluster in TiO<sub>2</sub> thin film [J]. *NanoStruc Mater*, 1999, 11: 195–201.
- [4] Akamatsu K, Tsuboi N, Hatakenake Y, et al. In situ spectroscopic and microscopic study on dispersion of Ag nanoparticles in polymer thin films [J]. *J Phys Chem, B*, 2000, 104: 10168–10173.
- [5] Lue Jui-Tzeng. A review of characterization and physical properties studies of metallic nanoparticles [J]. *J Phys Chem Solids*, 2001, 62: 1599–1612.
- [6] Dawson A, Prashant V. Kamat. Semiconductor-metal nanocomposites photoinduced fusion and photocatalysis of gold-capped TiO<sub>2</sub> (TiO<sub>2</sub>/Gold) nanoparticles [J]. *J Phys Chem, B*, 2001, 105: 960–966.
- [7] Gholinia A, Leach C. The production of small colloidal silver particles in SiO<sub>2</sub> sol-gel glass layers [J]. *Journal of Materials Science*, 1997, 32: 6625–6628.
- [8] Hornyak G L, Phani K L N, Kunkel D L, et al. Fabrication, characterization and optical theory of aluminum nanometal/nanoporous membrane thin film composites [J]. *NanoStruc Mater*, 1995, 6: 839–842.
- [9] Chatterjee A, Chakravorty D. Electrical conduction in sol-gel derived glass-metal nanocomposites [J]. *J Phys D: Appl Phys*, 1990, 23: 1097–1102.
- [10] JOSE-Yacamán M. The role of nanosized particles: a frontier in modern materials science, from nanoelectronics to environmental problems [J]. *Metallurgical and Materials Transactions*, 1998, A29: 713–725.
- [11] de Juan F, Ruiz-Hitzky E. Selective functionalization of mesoporous silica [J]. *Adv Mater*, 2000, 12: 430–432.
- [12] OH S-T. Fabrication of nanosized Ni-Co alloy-dispersed alumina nanocomposite [J]. *Journal of Materials Science Letters*, 1998, 17: 1925–1927.
- [13] Lee Kyung-Bok, Lee Sang-Min, Cheon Jir-Woo. Size-controlled synthesis of Pd nanowires using a mesoporous silica template via chemical vapor infiltration [J]. *Adv Mater*, 2001, 13: 517–574.
- [14] Shull R D. Change in magnetic state of Fe+ silica gel nanocomposites due to low temperature treatment in ammonia [J]. *J Appl Phys*, 1994, 75: 6840–6842.
- [15] Hornyak G L, Patrissi C J, Oberhauser E B. Effective medium theory characterization of Au/Ag nanoalloy-porous alumina composites [J]. *NanoStruc Mater*, 1997, 9: 571–574.
- [16] Arul Dhas N, Gedanken A. Sonochemical preparation and properties of nanostructured palladium metallic clusters [J]. *J Mater Chem*, 1998, 8: 445–450.

- [17] Dire S, Ceccato R, Facchin G, et al. Synthesis of Ni metal particles by reaction between bis (cyclooctadiene) nickel (0) and sol-gel  $\text{SiO}_2$  modified with SiH groups [J]. *J Mater Chem*, 2001, 11: 678 - 683.
- [18] Murakata A, Sato S, Ohgawara T, et al. Control of pore size distribution of silica gel through sol-gel process using inorganic salts and surfacants as additives [J]. *J Mater Sci*, 1996, 27: 1567 - 1574.
- [19] Dapurkar S E, Selvam P. Encapsulation of  $\text{Fe}_2\text{O}_3$  nanoparticles in periodic mesoporous materials [J]. *Mater Phys Mech*, 2001, 4: 13 - 16.
- [20] Boccuzzi F, Chiorino A, Manzoli M. Au/ $\text{TiO}_2$  nanostructured catalyst: effects of gold particle size on CO oxidation at 90K [J]. *Mater Sci Eng C*, 2001, 15: 215 - 217.
- [21] Okitsu K, Yue A, Tanabe S, et al. Sonochemical preparation and catalytic behavior of highly dispersed palladium nanoparticles on alumina [J]. *Chem Mater*, 2000, 12: 3006 - 3011.
- [22] Eriksson M. Hydrogen adsorption states at the Pd/ $\text{SiO}_2$  interface and simulation of the response of a Pd metal-oxide-semiconductor hydrogen sensor [J]. *Journal of Applied Physics*, 1998, 83: 3947 - 3951.
- [23] Fricke J.  $\text{SiO}_2$ -aerogels: Modification and Applications [J]. *J Non-Cryst Solids*, 1990, 121: 188 - 192.
- [24] Walker G S, Williams E, Bhattacharya A K. Preparation and characterization of high surface area alumina-tritania solid acids journal of materials science [J]. 1997, 32: 5583 - 5592.
- [25] SHEN Zhong, WANG Guoting. *Collide and Surface Chemistry* [M]. Beijing: Chemical Industry Press, 1997. 67 - 71. (in Chinese)
- [26] Altamirano-Juarez D C, Carrera-Figueiras C, Garinica-Romo M G, et al. Effects of metals on the structure of heat-treated sol-gel  $\text{SiO}_2$  glasses [J]. *J Phys Chem Solids*, 2001, 62: 1911 - 1917.
- [27] WU Yucheng. *The Physical Properties and Characterization of Nanocomposites with Transition Metals Assembled Into Mesoporous Silica* [M]. Hefei: ISSP, Chinese Academy of Sciences, 2000, 87 - 91. (in Chinese)
- [28] Parvathy N N, Pajonk G M, Venkateswara Rao A. Synthesis of various size CdS nanocrystals in porous silica matrix and their spectral and physical properties [J]. *NanoStruct Mater*, 1997, 8: 929 - 943.

( Edited by HE Xue-feng )